

Thermal and Fast Reactor Benchmark Tests of JENDL-3T

Hideki Takano and Kunio Kaneko

Department of Reactor Engineering
Japan Atomic Energy Research Institute, Tokai, Ibaraki, Japan

Abstract: Benchmark tests of JENDL-3T data were performed by analysing a lot of critical experiments for thermal and fast reactors, and the results were compared with those obtained using JENDL-2 data. The calculated results are summarized as follows:

(1) Thermal reactors: In U-235 fuel cores, the k_{eff} calculated with JENDL-3T cross sections increased about 0.3 % with respect to the JENDL-2 based values. The increase reflects the 0.24 % increase in $\nu(U-235)$ at the 2200m/sec. In Pu-239 fuel cores, the k_{eff} calculated with JENDL-3T data decrease about 0.6 % with respect to the JENDL-2 values, and the overprediction by JENDL-2 is improved. In U-233 fuel cores, the k_{eff} obtained with JENDL-3T data decrease about 1 % with respect to JENDL-2 values, and gives good agreement with the experiments.

(2) Fast reactors: The k_{eff} calculated with JENDL-3T data is overestimated for U-fuel cores and underestimated for Pu-fuel cores. The reaction rate ratios of Pu239(n,f)/U235(n,f) are in a good agreement with the experimental values, though U238(n,c)/Pu239(n,f) and U238(n,f)/U235(n,f) are overestimated. Moreover, the sodium void reactivity is in a good agreement with the experiments, and this is compared with overprediction of that obtained with JENDL-2 data.

(benchmark test, JENDL-3T, thermal reactor, high-conversion light water reactor, fast reactor, effective multiplication factor, reaction rate ratio, sodium void reactivity, Doppler reactivity, reaction rate distribution)

Introduction

A temporary nuclear data file JENDL-3T¹⁾ has been generated for testing an evaluated data file of JENDL-3. To assess the adequacy of JENDL-3T data for use in nuclear reactor design and applications, benchmark calculations are required for a number of critical experiments for thermal and fast reactors.

The calculations for thermal and high conversion light water reactors (HCLWR) are performed with SRAC²⁾ code system. The selected benchmark cores are a number of critical experiments with different fuels of U-235, U-233 and Pu-239, two water-moderated lattice (TRX-1 and 2)³⁾, two heavy water-moderated cores (ETA-1 and 2)⁴⁾ and a large number of uniform water-moderated lattices collected by Strawbridge and Barry⁵⁾. The PROTEUS cores are selected for the HCLWR benchmarks.

Fast reactor benchmark calculations are performed for twenty-two benchmark cores selected from the ZPR, ZPPR, FCA, ZEBRA, SNEAK and VERA critical experiment series. These calculations are based on one and two dimensional diffusion theories.

Benchmark Testing CoresThermal Reactor

A variety of critical and lattice experiments were selected as follows: The ORNL series³⁾ are unreflected spheres of uranyl nitrate in H₂O. The ratio-ranges of H/U-235 are from 972 to 1835. The critical experiments selected by McNeaney and Jenkins⁶⁾ contain the high enriched U-235 and U-233 with the ratio-ranges of H/U from 0 to 1400. There are two experiments including U-233 and Th-232 fuels. The PNL 1 - 5 series³⁾ are homogeneous aqueous plutonium nitrate experiments with the H/Pu-239 ratio ranging from 131 to 1204.

The uniform water-moderated lattice experiments collected by Strawbridge and Barry⁵⁾ contain 61 U-metal and 55 UO₂-rods lattices covering a wide range of parameters.

Lattice parameters are measured in the TRX³⁾ and ETA⁴⁾ cores. The TRX-1 and 2 represent fully reflected fuel rods of enriched 1.3 % uranium, aluminum-clad and H₂O-moderated. The ETA-1 and 2 are tight Th-U235 and Th-U233 lattices moderated with heavy water.

HCLWR

The PROTEUS series⁷⁾ are tight lattice experiments with the moderator-to-fuel volume ratio of 0.5 for high conversion light water reactors. The fissile plutonium enrichments are about 6 and 8 % for the cores (1, 2 and 3) and (4, 5 and 6), respectively. Three different H₂O-voidage states were measured, viz. 0, 42.5 and 100 % void, to check the void coefficient.

Fast Reactor

Fast reactor benchmark cores consist of 17 benchmark assemblies collected for ENDF/B-IV data testing³⁾, the JOYO and MONJU mock-up cores (FCA-V-2 and FCA-VI-2), MORZART cores (MZA and MZB) and the JUPITER reference core (ZPPR-9). These have a wide variety from 12 to 4600 liter of core sizes, from zero to eight concentration ratios of fertile to fissile in core, and of 15 plutonium and 7 uranium fuel cores as shown in Table 1.

Benchmark Calculations

Benchmark experiments were analysed with SRAC using two cross section libraries SRACLIB-JENDL2 and -JENDL3T based on JENDL-2 and JENDL-3T data, respectively. These libraries were produced with the processing codes, TIMS-PGG⁸⁾ and SRACLIB²⁾. The RESENDD code was used to treat the Reich-Moore resonance formula for Pu-239. This library contained 74-group constants for fast energy region and 48-group constants for thermal energy region. In resonance energy region, a ultra-fine group library was prepared for some important heavy resonant nuclides. Cell spectrum calculations were performed by the collision probability method. The

Table 1 Fast critical benchmark cores

Assembly	fuel	volume (l)	N8/N9 or N5
VERA-11A	Pu	12	0.05
ZEBRA-3	Pu	50	8.5
SNEAK-7A	Pu	110	3.0
FCA-5-2	Pu	200	2.3
ZPR-3-53	Pu	220	1.6
SNEAK-7B	Pu	310	7.0
ZPR-3-50	Pu	340	4.5
ZPR-3-48	Pu	410	4.5
ZPR-3-49	Pu	450	4.5
ZPR-3-56B	Pu	510	4.5
MZA	Pu	570	3.9
FCA-6-2*	Pu	630	6.6
MZB	Pu	1800	5.8
ZPPR-2	Pu	2400	5.5
ZPR-6-7	Pu	3100	6.5
ZPPR-9*	PU	4600	9.4
VERA-1B	U	30	0.07
ZPR-3-6F	U	50	1.1
ZPR-3-12	U	100	3.8
ZPR-3-11	U	140	7.5
ZEBRA-2	U	430	6.2
ZPR-6-6A	U	4000	5.0

* Two-dimensional benchmark core

ultra-fine group method was used in the resonance region below 130 eV. Criticality calculations were performed with P_1 - S_8 approximation by a one-dimensional S_n -transport code ANISN.

The fast reactor benchmark calculations for k_{eff} and reaction rate ratios were performed with one-dimensional diffusion and transport codes. Reaction rate distributions, Doppler and Na-void reactivities for ZPPR-9 and FCA-VI-2 cores were calculated by two-dimensional diffusion theory. For these calculations, a JFS3-JENDL3T library with 70-group structure was produced by TIMS-PGG processing code.

Results and Discussions

Thermal Cores of U-235 Fuel

Figure 1 shows the k_{eff} obtained for ORNL and McNeany-Jenkins cores as a function of the atomic ratio of H/U-235. The results are underestimated with increase of H/U-235 ratio. The k_{eff} calculated for 116 cases of Strawbridge and Barry were as follows: The averaged k_{eff} obtained for UO_2 -rod lattice cases was 0.991 for JENDL-3T and 0.983 for JENDL-2. The averaged k_{eff} for U-metal rods are 0.992 and for JENDL-3T and 0.989 for JENDL-2, respectively. It is main reason for these differences that the ν -value of U-235 for JENDL-3T is 0.24 % larger than JENDL-2 data at the 2200 m/sec. Integral lattice parameters were calculated for the TRX-1 and 2 cores, and ρ_{28} and δ_{28} for JENDL-3T were overestimated by 6 - 9 %.

Thermal Cores of U-233 Fuel

Figure 2 shows the multiplication factors calculated for McNeany-Jenkins cores as a function of the ratio H/U-233. The results obtained by JENDL-3T data become about 1.0 % smaller than those by JENDL-2 data and give good agreement with experiments.

The integral parameters ρ_{02} , CR, CR' and δ_{02} calculated for the ETA-1 and 2 cores using JENDL-3T data were significantly improved over corresponding analyses using JENDL-2 data⁹⁾. This reason is that Th-232 capture cross sections of JENDL-3T are significantly larger than JENDL-2 data in the resonance region below 200 eV.

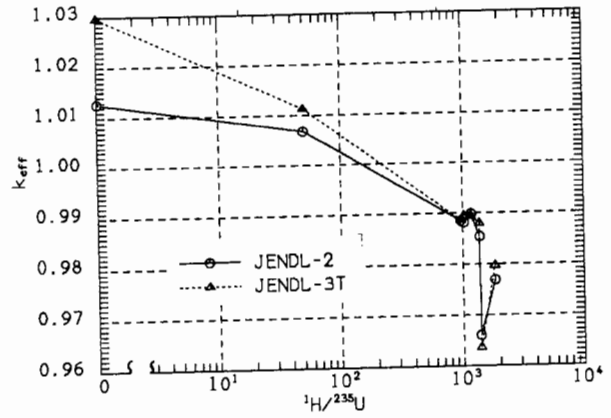


Fig.1 k_{eff} for ^{235}U fuel cores (ANISN, P_1S_8)

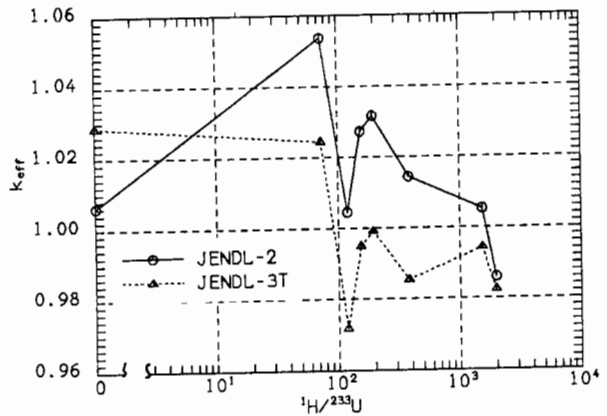


Fig.2 k_{eff} for ^{233}U fuel cores (ANISN, P_1S_8)

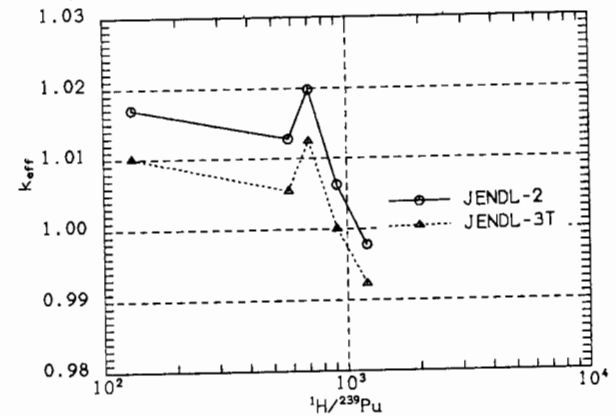


Fig.3 k_{eff} for ^{239}Pu fuel cores (ANISN, P_1S_8)

Thermal Cores of Pu-239 Fuel

The calculated k_{eff} 's are shown as a function of the ratio H/Pu-239 in Fig.3. The k_{eff} obtained using JENDL-3T data are about 0.6 % smaller than those using JENDL-2 data, and the overprediction by JENDL-2 is improved. Figure 4 shows the deviation of the Pu-239 fission cross sections for JENDL-3T from those of JENDL-2. It is observed that the fission cross sections of JENDL-3T are significantly smaller than JENDL-2 data in many energy groups. This causes the decrease of k_{eff} obtained using JENDL-3T data.

HCLWR PROTEUS Cores

The results calculated for PROTEUS cores 1 - 3 are shown as a function of the coolant void fraction (%) in Figs.5 and 6. The k-infinity using JENDL-3T gives very good agreement with experi-

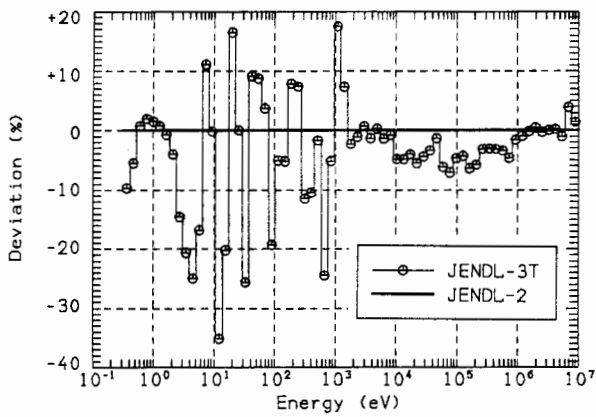


Fig. 4 Deviation for $\sigma_c(^{239}\text{Pu})$ of JENDL-3T from JENDL-2

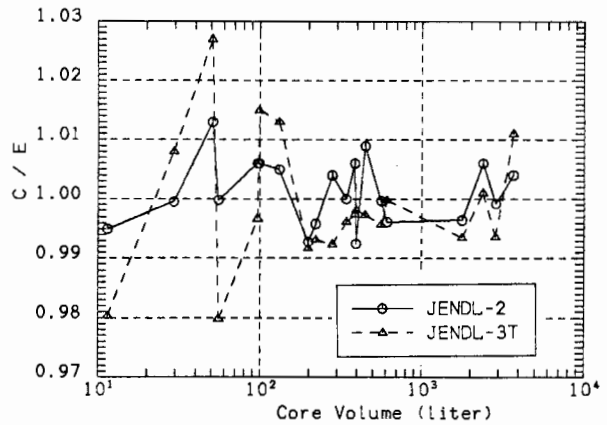


Fig. 7 k_{eff} for fast critical cores

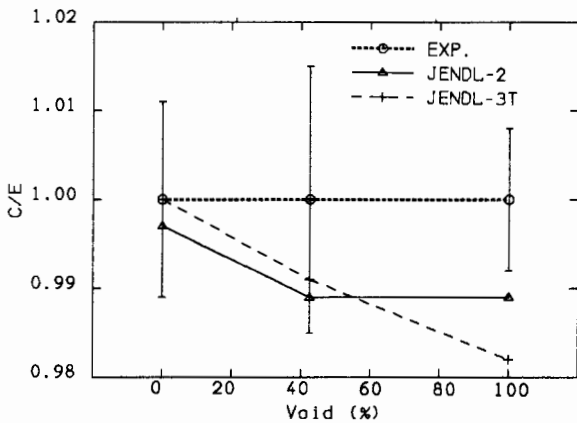


Fig. 5 Comparison of k_{∞} for PROTEUS cores

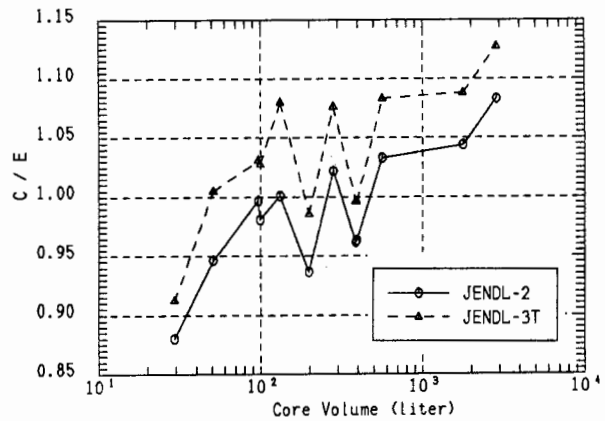


Fig. 8 C/E values of $\langle \sigma_c / \sigma_f \rangle$

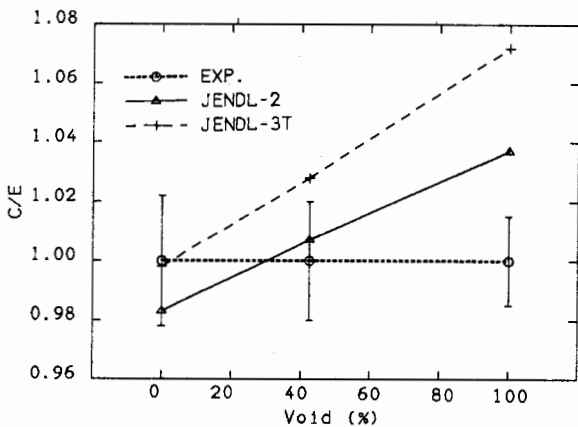


Fig. 6 $U^{238}(n,\gamma)/Pu^{239}(n,f)$ for PROTEUS cores

ments in the zero void state as seen in Fig. 5. However, the k_{∞} of JENDL-3T depend stronger than that of JENDL-2 on coolant voidage states.

Figure 6 shows the comparison of reaction rate ratio $U^{238}(n,\gamma)/Pu^{239}(n,f)$ (C8/F9) corresponding to conversion ratio. The results using JENDL-3T are about 2% larger than those using JENDL-2.

In $U^{238}(n,f)/Pu^{239}(n,f)$ (F8/F9) for threshold fission reaction rate, the results using JENDL-3T increased still more the overprediction obtained by JENDL-2 for the experimental values.

Fast Critical Assemblies

One-dimensional benchmark calculations were performed for 20 benchmark cores as shown in Table 1. The k_{eff} obtained with the JENDL-3T data are overestimated for uranium cores and are und-

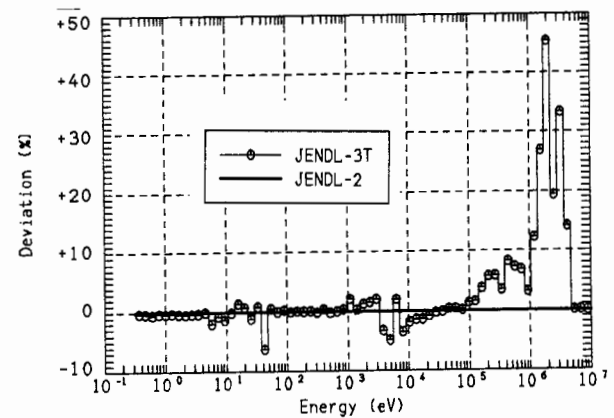


Fig. 9 Deviation for $\sigma_c(^{238}\text{U})$ of JENDL-3T from JENDL-2

erestimated for plutonium cores as shown in Fig. 7. The overestimate for uranium cores is due to a large $\nu(U-235)$ -value evaluated for JENDL-3T, and the underestimate for plutonium cores is due to smaller $Pu-239$ fission cross sections as shown in Fig. 4. The JENDL-3T data are smaller 5% than the JENDL-2 data in the energy range from 10 KeV to 1 MeV. This causes 1.7% reduction of k_{eff} for Pu-cores and about 4% increase for C8/F9. In the resolved resonance region below 1 KeV, the JENDL-3T data smaller than JENDL-2 data. This may be important problem for coolant void reactivity analysis in HCLWR and LMFBR.

The central reaction rate ratio C8/F9 or C8/F5 obtained by JENDL-3T are larger than those for JENDL-2. The results obtained for C8/F9 are compared in Fig. 8.

Figure 9 shows the deviation for U-238 capture cross sections of JENDL-3T from JENDL-2 data. There is considerable discrepancy in the

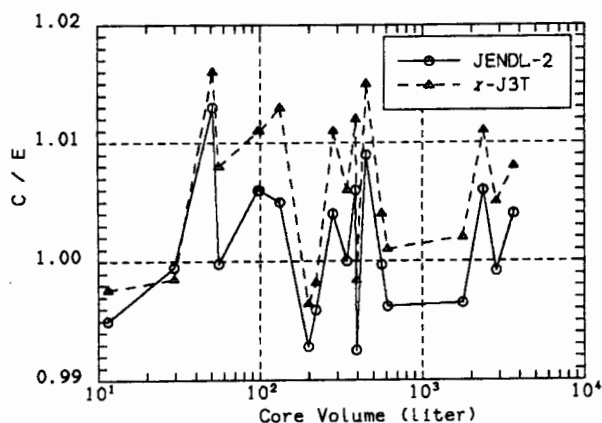


Fig. 10 The effect of fission spectrum change on K_{eff}

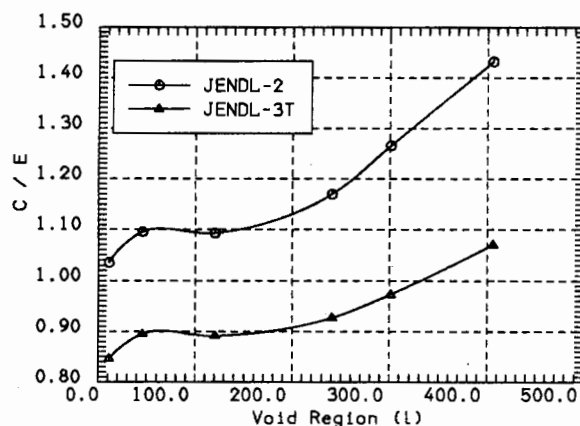


Fig. 12 Comparison of Na-void reactivity at the ZPPR-9 core

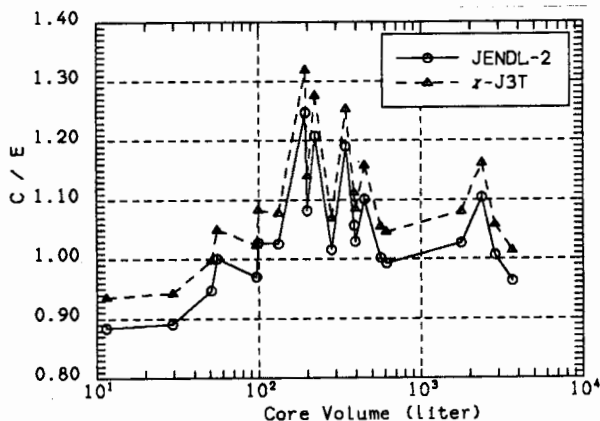


Fig. 11 The effect of α change on $\langle \sigma_f^{238} / \sigma_f^{235} \rangle$

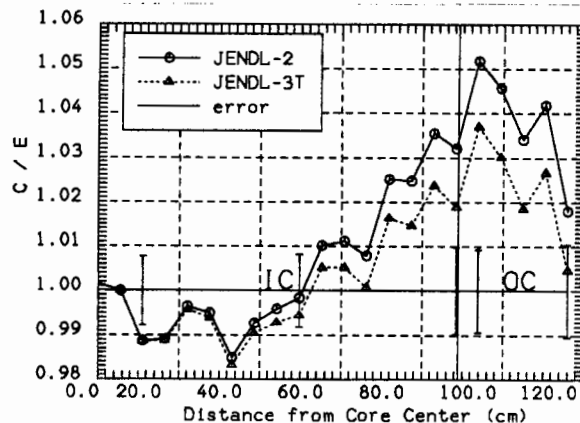


Fig. 13 ^{239}Pu fission rate distribution at the ZPPR-9 core

Table 2 NUO₂ Doppler reactivity calculated for ZPPR-9 assembly

Temperature (k)	Calculation/Experiment	
	JENDL-2	JENDL-3T
298 - 487	0.879	0.938
298 - 644	0.886	0.947
298 - 794	0.858	0.918
298 - 935	0.896	0.959
298 - 1087	0.888	0.951

energy range above 100 KeV. This causes 0.3 - 0.8 reduction of k_{eff} and 3 % increase of C8/F9.

In JENDL-3T, fission spectrum was evaluated on the basis of Madland-Nix formula, and it is harder than that of JENDL-2. The k_{eff} calculated with this harder spectrum becomes larger 0.5 % than the result of JENDL-2, and the threshold reaction rate ratio F8/F5 also becomes larger by 5 %, as observed from Figs. 10 and 11.

The F9/F5 calculated by JENDL-3T improve the underprediction observed for the results obtained with JENDL-2. This may be an important reason that the fission cross sections for Pu-239 and U-235 were evaluated on the basis of a simultaneous evaluation method.

Two-dimensional benchmark calculations were performed for ZPPR-9 and FCA-VI-2 assemblies to assess Doppler reactivity, sodium reactivity worth and reaction rate distribution. The overestimation for sodium void worth obtained by JENDL-2 is remarkably improved by JENDL-3T as seen in Fig. 12. The NUO₂ Doppler worth calculated with JENDL-3T is increased by about 6 % in the comparison with those for JENDL-2 and is in good agreement with the experiments as shown in Table 2. The reaction rate distribution in the outer core region is also improved by about 1.0 % as observed from Fig. 13.

Concluding Remarks

The benchmark calculation results using JENDL-3T are summarized as follows: In thermal reactor benchmark tests, the k_{eff} s obtained with the JENDL-3T data were in good agreement with the experiments, though it was observed that they depend considerably on the ratio of H/U. In fast reactor benchmarks, the k_{eff} calculated with the JENDL-3T data was overestimated for U-cores and underpredicted for Pu-cores. The reaction rate ratios of C8/F9 and F8/F9 were overestimated for the JENDL-3T data. On the other hand, Doppler and sodium void reactivities, and reaction rate distribution obtained for the JENDL-2 data were significantly improved by using the JENDL-3T data.

The present benchmark tests of JENDL-3T showed that nuclear data to be reevaluated are ν , fission cross section and fission spectrum for U-235, fission cross section and fission spectrum for Pu-239, and capture and inelastic scattering cross section for U-238 until the final compilation of JENDL-3.

REFERENCES

1. JENDL Compilation Group (Nuclear Data Center, JAERI): JENDL-3T, Private communication (1987).
2. K. Tsuchihashi et al.: JAERI 1285 (1983) and 1302 (1987).
3. "Cross Section Evaluation Working Group Benchmark Specifications," ENDF-202 (BNL-19302).
4. J. Hardy et al.: Nucl. Sci. Eng., 55, 401 (1974).
5. L.E. Strawbridge and R.F. Barry: Nucl. Sci. Eng., 23, 58 (1965).
6. S. McNeany and D. Jenkins: Nucl. Sci. Eng., 65, 441 (1978).
7. R. Chawla et al.: NUREG/CP-0034, 902 (1982).
8. H. Takano et al.: JAERI-M82-072 (1982).
9. H. Takano and K. Kaneko: JAERI-M 88-065 (1988).